THE IMPACT OF Ca/P RATIO AND pH ON SYNTHESIS OF HYDROXYAPATITE AND ITS THERMAL BEHAVIOUR

Lenka ŠIMKOVÁ, Petra ŠULCOVÁ

Department of Inorganic Technology, Faculty of Chemical Technology, University of Pardubice, Doubravice 41, 532 10 Pardubice, Czech Republic
E-mail: lenka.simkova1@student.upce.cz

INTRODUCTION

The cause of the extension of phosphate pigments nowadays is more stringent environmental and hygienic limits, which require for the replacement of toxic lead and chromate pigments with nontoxic but very effective pigments [1]. Hydroxyapatite (HAP, $Ca_{10}(PO_4)_6(OH)_2$) is the main inorganic compound of hard tissues such as bones and teeth of vertebrate animals and humans. Consequently, HAP was easily considered as a bioactive material for synthetic bone substitution due to its biocompatibility, and chemical and biological affinity with bony tissue [2].

The main applications of hydroxyapatite are its use as a coating of metallic prostheses, which has two important functions: to protect the implant against corrosion and to improve implant's biocompatibility with the human body [3]. Since hydroxyapatite is very suitable and useful for the protection of implants against corrosion it can be very functional even for steel protection like do other phosphate pigments [4].

It is known that the optimum Ca/P molar ratio must be 1.667. However one of the main problems related to HAP processing is the low stability of HAP at temperatures near to the sintering range, which is attributed to deviations from the ideal Ca/P ratio [5]. In addition, a lot of factors contribute to complicating the picture: particle size, sample structure, purity, powders surface condition, and even particles aggregation can support undesirable decompositions and phase transitions. Particularly the formation of β-TCP ($Ca_3(PO_4)_2$) as the most likely phenomenon in the decomposition process highlights the importance of the Ca/P ratio in the control of HAP stability [6].

In the present work, the preparation of HAP under different synthesis condition (Ca/P ratio and pH) has been implemented and their characteristics studied, in particular, phase composition, morphology and thermal stability in relation to Ca/P ratio have been focused.

EXPERIMENTAL PART

In order to select suitable synthesis conditions for the formation of hydroxyapatite phase, the thermodynamic stability of the hydroxyapatite $Ca_{10}(PO_4)_6(OH)_2$ in aqueous solution was analysed and approved in laboratory conditions. Figure 1 shows the predominance area diagram for the Ca^{2+} - PO_4^{3-} water system at 25 °C. The x-axis shows a pH scale ranging from 0 to 14 and the y-axis shows the decimal logarithm of the phosphate ions concentration. From the figure it is obvious that hydroxyapatite is stable in the pH range from 4.8 to 14.
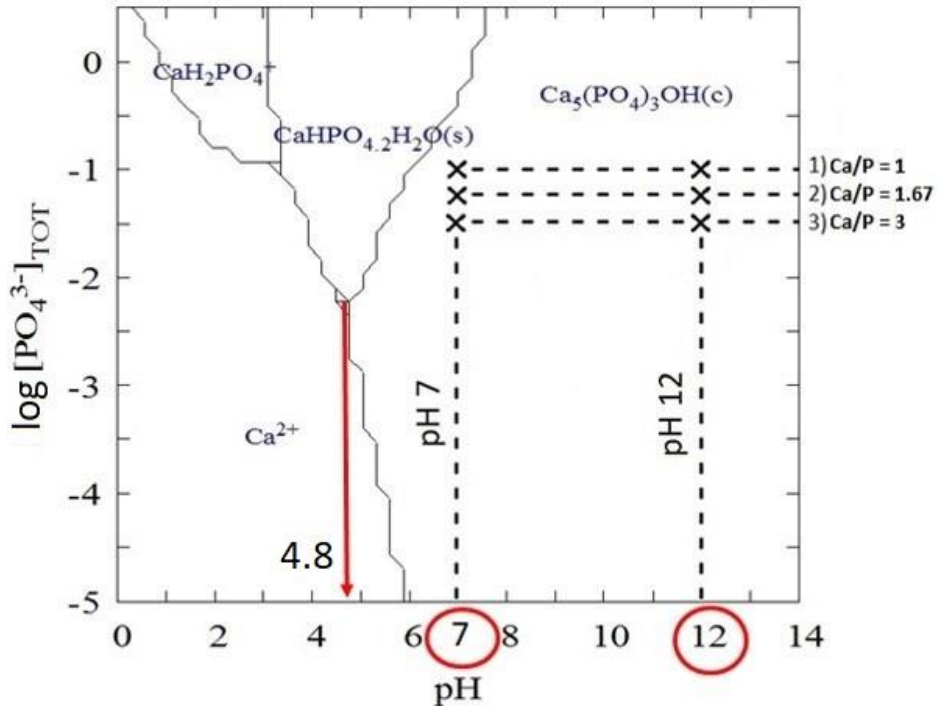
Figure 1: Predominance area diagram for the Ca^{2+}- PO_4^{3-} system.

Due to this information, three Ca/P ratios were chosen for the synthesis of hydroxyapatite, which were studied at pH = 7 and pH = 12 based on the area of the hydroxyapatite form:

- Ca/P = 1; in this case, HAP formation occurs in excess of phosphate ions;
- Ca/P = 1.67; this corresponds to the Ca/P stoichiometry of hydroxyapatite, which is 10/6;
- Ca/P = 3; HAP formation occurs in excess of calcium ions.

The selected suitable precipitation conditions (Ca/P=1, 1.67, 3; pH=7, 12) were adjusted to synthesize pure hydroxyapatite to form $Ca_{10}(PO_4)_6(OH)_2$. For the synthesis of powders, 1M solutions of starting compounds ($Ca(NO_3)_2 \cdot 4H_2O$, $(NH_4)H_2PO_4$) were prepared. The precise concentrations of these solutions were determined using analytical methods (titration, gravimetric and photometric analyses). Altogether, 12 samples were synthesized at different synthesis conditions (Table 1, precipitation rate 2 ml/min).The prepared powders were aged during 24 hours, filtered and washed with distilled water to neutral pH, then dried at 80 °C for 6 h.

The phase analysis of the powdered materials was studied by X-ray diffraction analysis (XRD). The phase composition was determined using diffractometer MiniFlex 600 (Rigaku, Japan) equipped with a vertical goniometer of 17 cm in the 2θ range of 10°–50°. The accuracy of goniometer was ±0.02°. X-ray tube with Cu anode (U = 40 kV, I = 15 mA) was used (CuKα radiation).The morphology of synthesized powders was studied by scanning electron microscopy (SEM). The morphology of the prepared powder was determined using an electron microscope equipped with an IXRF Systems analyzer and a Gresham Sirius 10 detector (Joel Inc., USA).The

thermal behavior of studied compounds was followed by simultaneous thermal analysis using the STA 449C Jupiter (NETZSCH, Germany) which allows simultaneous registration of the thermoanalytical curves TG and DTA. The measurements were provided at temperature interval from 30 to 1200 °C with heating rate 10 °C·min^{-1}. The samples were measured in portions approx. 60 mg.

Table 1: Overview of the obtained samples and the synthesis conditions

Sample	Ca/P ratio	pH
1	1	7
2	1.67	7
3	3	7

RESULTS AND DISCUSSION

Effect of synthesis conditions (Ca/P ratio, pH) on hydroxyapatite formation

According to a result of the SEM analysis of synthesized samples, hydroxyapatite phase was formed as nanocrystalline whose the size and shape of crystals depend on the Ca/P ratio (Ca/P = 1 needle-shaped shapes are identified, Ca/P = 1.67 – tabular plates, Ca/P = 3 - different needle-like shapes, tabular plates, and bulky formations) and pH (pH = 7 - larger and thinner particles, pH = 12 - larger and smaller particles) and does not depend on the precipitation rate.

The phase composition of the samples was determined by XRD analysis. Two distinct structures of hydroxyapatite have been identified: monoclinic and hexagonal. Figure 2 shows the diffractogram of sample 1 containing the hydroxyapatite diffraction line $Ca_{10}(PO_4)_6(OH)_2$ with the following parameters: hexagonal crystalline system; space group $P6_3/m$. Figure 2 also shows a diffractogram of sample 2 containing the hydroxyapatite diffraction line $Ca_{10}(PO_4)_6(OH)_2$ with the following parameters: monoclinic crystalline system; space group $P2_1/b$. These structural types of hydroxyapatite were selected based on the lowest value of FOM (figure of merit), i.e., based on the best match. Comparison of the crystal size results obtained from SEM and XRD analysis revealed that the minimum dimensions of SEM analysis were comparable to the maximum dimensions of XRD analysis. In general, SEM analysis shows a larger crystal size. This phenomenon can be explained by the fact that for the maximum crystal size analysis the largest particles that are visible in the SEM images are selected. The contributions of these largest particles to the average crystal size are small. Further, this phenomenon can be explained by the fact that the largest crystals visible in the SEM figures are made up of smaller crystals.
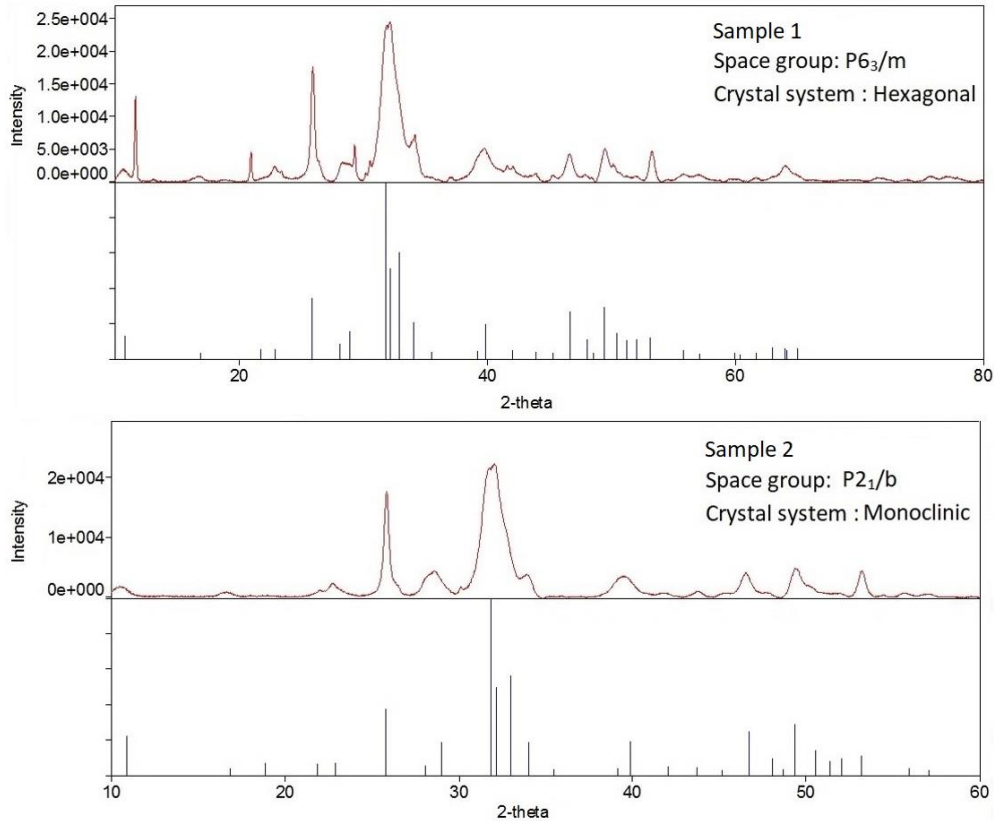
Figure 2 : Diffractogram of crystal system of hydroxyapatite

Effect of synthesis conditions on thermal behavior of hydroxyapatite

By DTA/TG analysis, the effect of Ca/P ratio was proven (Figure 3, Table 2). There is consensus that the thermal behavior of HA occurs in a 4 step process involving dehydroxylation and decomposition:

- Step 1: $Ca_{10}(PO_4)_6(OH)_2 \rightarrow Ca_{10}(PO_4)_6(OH)_{2-2x}O_x\square_x + x\ H_2O$
  (hydroxyapatite)   (oxyhydroxyapatite)
- Step 2: $Ca_{10}(PO_4)_6(OH)_{2-2x}O_x\square_x \rightarrow Ca_{10}(PO_4)_6O + (1-x)\ H_2O$
  (oxyhydroxyapatite)   (oxyapatite)
- Step 3: $Ca_{10}(PO_4)_6O \rightarrow 2\ Ca_3(PO_4)_2 \qquad + \qquad Ca_4(PO_4)_2O$
  (oxyapatite)   (tricalcium phosphate)   (tetracalcium phosphate)
- Step 4: $Ca_4(PO_4)_2O \rightarrow 4\ CaO + P_2O_5 \uparrow$ or $Ca_3(PO_4)_2 \rightarrow 3\ CaO + P_2O_5\uparrow$

Dehydroxylation includes the loss of water, which proceeds via the provisional formation of firstly oxyhydroxyapatite (OHAP) and then oxyapatite (OHA) where $\square$ stands for a lattice vacancy in the OH position along the crystallographic c-axis. Decomposition of OHA then proceeds to secondary phases such as tricalcium phosphate (β-TCP) and tetracalcium phosphate (T-TCP). The transformation of HA has important consequences in bone engineering and plasma coated implants, since β-TCP is a resorbable calcium phosphate, and while it will enhance resorption of HA implants, decomposition of HA will also reduce the mechanical properties of the material [7].
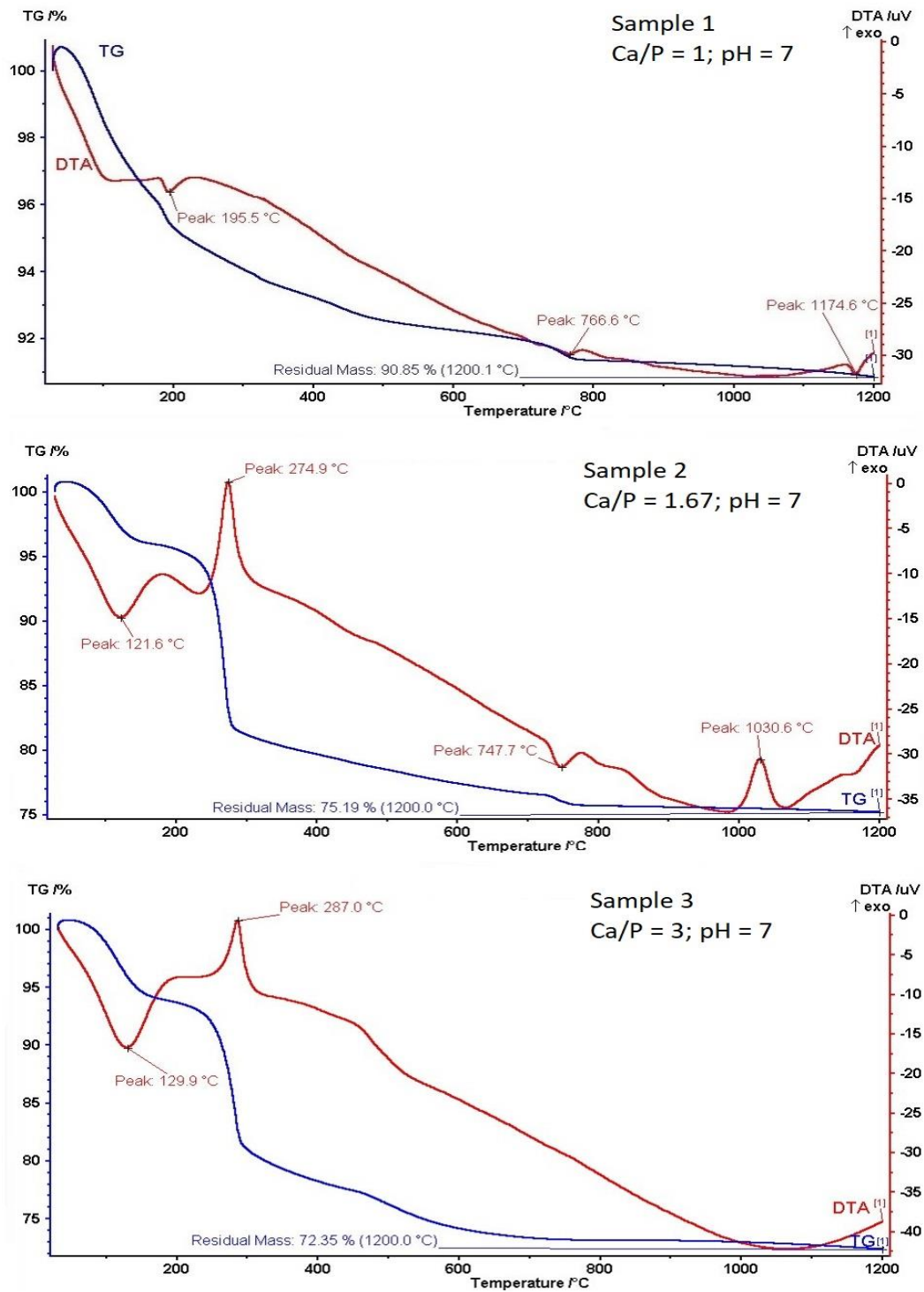
Figure 3: Thermal behavior of hydroxyapatite

Table 2: Overview of processes occurring during hydroxyapatite decomposition

Sample	TA results				Total Δm [%]	Process
	T range [°C]	Δm [%]	TA effect	Tpeak [°C]		
1	80-350	5.05	endo	196	9.15	dehydration
	600-900	1.15	endo	767		dehydroxylation with the formation of OHAP→OHA
	1000-1200	0.73	endo	1175		OHA decomposes to form β-TCP and T-TCP
2	70-180	3.87	endo	122	24.81	dehydration
	180-500	14.94	exo	275		elimination of ammonia; dehydroxylation with the formation of OHAP → OHA
	550-800	5.49	endo	748		OHA decomposes to form β-TCP and T-TCP
	900-1050	-	exo	1031		decomposition of T-TCP in CaO and $Ca_3(PO_4)_2$
3	80-180	5.92	endo	130	27.65	dehydration
	180-330	13.87	exo	287		elimination of ammonia
	350-800	6.87	-	-		unidentified

CONCLUSION

The selected synthesis conditions are suitable for the formation of crystalline hydroxyapatite phase. By SEM analysis, the effect of Ca/P ratio on sample particles was proven (different shape and size). The phase composition of the samples was determined by XRD analysis (two distinct structures have been identified: hexagonal and monoclinic). By DTA/TG analysis, the effect of Ca/P ratio was proven. Thermal behavior of HA occurs in a 4 step process involving dehydroxylation and decomposition. Decomposition of OHA then proceeds to secondary phases such as tricalcium phosphate (β-TCP) and tetracalcium phosphate (T-TCP).

LITERATURE

[1] Kalendová A.: Technologie nátěrových hmot I, Univerzita Pardubice (2003).
[2] Jarcho M, Bolen C.H, Thomas M.B, Bobick J, Kay J.F, Doremus R.H.: J Mater Sci. 11 (1976) 2027.
[3] Huang Y, Hao M, Nian X.: Ceramics Int. 42 (2016) 11876.
[4] Gorodylova N, Dohnalová Ž, Šulcová P. et.al.: Prog Org Coat. 93 (2016) 77.
[5] Wang P.E, Chaki T.K.: J Mater Sci-Mater M. 4 (1993) 150.
[6] Tampieri A, Celotti G, Szontagh F, Landi E.: J Mater Sci-Mater M. 8 (1997) 29.
[7] Chetty A, Wepener I, Marei M.K.: Nov Scie Publis. 1 (2013) 164.